INTERNATIONAL JOURNAL OF COMMUNICATIONS
Issue 3, Volume 5, 2011

Blind Channel Equalization in Impulse Noise

Rubaiyat Yasmin and Tetsuya Shimamura
Graduate School of Science and Engineering, Saitama University
255 Shimo-okubo, Sakura-ku, Saitama 338-8570, Japan
yasmin@sie.ics.saitama-u.ac.jp

Abstract- This paper presents a robust blind channel equalization technique in impulse noise environments. To suppress impulse noise effectively, the combination of order statistics (OS) and adaptive thresholding is considered. We implement nonlinear adaptation with the OS operation based on the Sato error criterion. The adaptive threshold is calculated using the variance of the input signal. Computer simulations demonstrate that a significant improvement in both the bit error rate and mean square error is achieved for communication channel models with a mixture of additive white Gaussian noise and impulse noise, in which two different impulse noise generation models with different noise generation probability are considered.

Keywords- Blind channel equalization, Impulse noise, Order statistics, Threshold

1 INTRODUCTION

Multipath fading is a serious problem which affects the reliability of communication systems such as mobile radio and high frequency (HF) channels. Such digital communication channels suffer from intersymbol interference (ISI) invoked from the multipath fading. To compensate for ISI, adaptive equalization techniques can be used [1]. Usually, the equalization techniques are training sequence based [2][3]. The communication capacity, however, degrades with the length of the training sequence. Hence, blind equalization [4] can be a solution to overcome such a situation, in which the equalizer works without any training sequence. Most of the blind equalizers use a linear adaptive algorithm (with a nonlinear error criterion) and assumes that the additive noise is Gaussian [5]. However, the Gaussian assumption of the noise is not always valid in practical communications systems, because sometimes the noise can be impulsive [6]. Linear filters may not be suitable there. A large amplitude of the impulse noise adversely affects both signal restoration and adaptation [7]. This has prompted a great deal of research in nonlinear filtering techniques that are more robust against impulse noise.

Order statistics (OS) filters are known for suppressing impulse noise [8]-[10]. The L-filter [8] forms a new input vector by sorting the elements of input vector. This filter works well in image processing, but it cannot perform well in channel equalization due to the loss of temporal information after the ranking operation. The Ll-filter [9] provides good signal reconstruction and noise removal by considering both time and rank orders. In [10], the performance of the Ll-filter was investigated for the purpose of (training based) channel equalization in the presence of impulse noise, and it was shown that the Ll-filter behaves better than the linear filter in terms of mean square error (MSE). The C-filter [11] also utilizes the rank and temporal information in processing inputs with impulse noise, which is also applicable to the channel equalization purpose. In [11], however, the task of channel equalization was not studied. On the other hand, the multirate optimizing order statistics equalizer (MOOSE) has a two-stage architecture, consisting of an order statistical impulse removal prefilter and a (training based) channel equalizer [12]. For the MOOSE, the use of the impulse removal prefilter does not provide inherently a solution to the equalization problem in impulse noise without the fractionally spaced technique. This is because the impulse removal prefilter is a general filter to suppress impulse noise, which is applicable to a variety of fields containing impulse noise. Like the above, there are several works about the training based equalization techniques in impulse noise. However, there are only a few works about blind equalization in impulse noise environments. In [13] the author presents an approach for blind channel equalization in impulse noise, which is based on the information theoretic learning method instead of the MSE method. The approach can suppress impulse noise well, but the resulting convergence is not satisfactory especially with respect to speed.

The Sato equalizer [14] is a pioneer work of blind equalization, which is a simple and effective blind equalizer and has been widely used for applications. The performance of the Sato equalizer in impulse

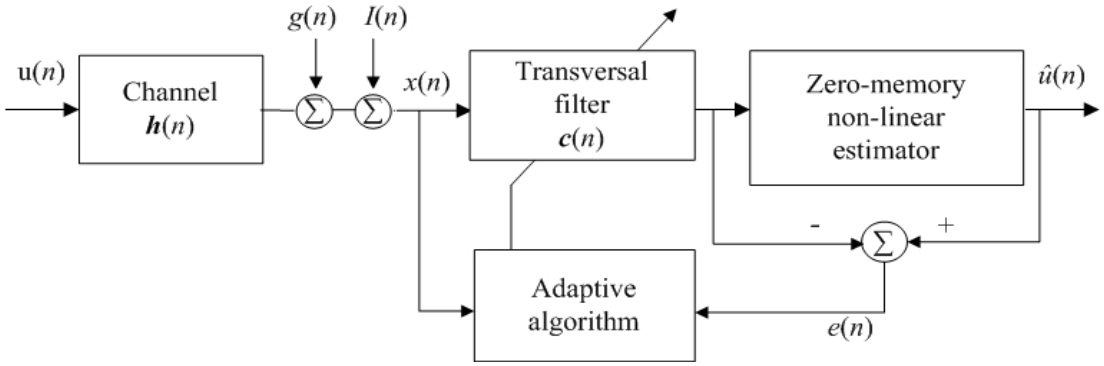

Figure 1: Blind channel equalization system with impulse noise

noise is not known. In this paper, we investigate the performance of the Sato equalizer in impulse noise and visualize that the Sato equalizer is severely affected in an impulse noise environment. In order to improve the performance of the Sato equalizer in impulse noise, we need to suppress the impulse noise effect in the adaptation process. One idea to accomplish this is to use the principle of the C-filter in the adaptation process of the Sato blind equalizer. From this point of view, we derive an OS based blind equalizer with the Sato error criterion, where the time and rank orders are taken into account.

An adaptive threshold technique has been used in the training based equalizer to handle significant outliers in [15]. This technique is also applicable to the blind equalizer. In this paper, we investigate the effectiveness of the adaptive threshold [15] for blind equalization with the Sato error criterion. The threshold is calculated with the variance of the input signal for each iteration. Unlike the trimming with the C-filter [11], the thresholding calculation is kept isolated from the adaptation process.

The organization of this paper is as follows. The channel model and blind equalization system to be considered in this paper are described in Section 2. The proposed OS based blind equalization with the Sato error criterion (OS-Sato) is described in Section 3. In Section 4, the adaptive threshold technique is described and a threshold based blind equalizer is derived. Section 5 describes noise generation models, and Section 6 shows computer simulation results to validate the proposed blind equalizers. Section 7 concludes the paper with a brief summary.

2 CHANNEL MODEL AND BLIND CHANNEL EQUALIZATION

We consider a digital communication system where the transmitted sequence is corrupted by both the additive white Gaussian noise (AWGN) and impulse noise. The channel is described by

$$x(n) = \sum_{i=0}^{L-1} h_i(n)u(n-i) + g(n) + I(n), \quad (1)$$

where $h_i(n), i = 0, 1, \cdots, L$ are the channel coefficients, $u(n)$ is the transmitted sequence, $g(n)$ is the AWGN, and $I(n)$ is the impulse noise. The transmitted sequence $u(n)$ is assumed to be an independent random binary sequence of ± 1 with an equal probability. For the mixture noise, the impulse noise $I(n)$ is added to the AWGN $g(n)$. The probability of the generation of the impulse noise $I(n)$ is defined by P_i.

Figure 1 shows a system model of the blind equalizer considered in this paper, where the Sato algorithm is employed as the adaptation scheme of the transversal filter, this corresponds to the so-called Sato equalizer. The Sato equalizer minimizes a non-convex cost function:

$$J = E[(\hat{u}(n) - y(n))^2], \quad (2)$$

where $\hat{u}(n)$ is an estimate of $u(n)$, which is given by

$$\hat{u}(n) = \gamma sgn[y(n)] \quad (3)$$

with the sign function $sgn[]$ returning the sign of its argument. The dispersion coefficient γ in (3) controls the output scaling, which is computed as

$$\gamma = \frac{E[u^2(n)]}{E[|u(n)|]}. \quad (4)$$

The Sato equalizer updates its coefficient vector by the least mean squares (LMS) algorithm. The adaptation equations are given by

$$y(n) = \mathbf{x}(n)^T \mathbf{c}(n), \quad (5)$$

$$e(n) = \hat{u}(n) - y(n) = \gamma sgn(y(n)) - y(n), \quad (6)$$

$$\mathbf{c}(n+1) = \mathbf{c}(n) + \mu e(n)\mathbf{x}(n)\cdot \quad (7)$$

where $\mathbf{x}(n) = [x(n), x(n-1), \cdots, x(n-L+1)]^T$ is the input vector, $\mathbf{c}(n) = [c(n), c(n-1), \cdots, c(n-L+1)]^T$ is the coefficient vector, and $e(n)$ is the estimation error. The parameter μ controls the convergence of the equalizer.

3 OS BASED BLIND EQUALIZATION

In this section, the proposed OS-Sato equalizer is described where the OS operation is incorporated into the Sato equalizer.

The adaptation of the OS-Sato equalizer is done based on the OS of the input vector, where a combination of temporal and rank orders information is used. The OS-Sato equalizer utilizes the filter output to estimate the transmitted sequence blindly with the Sato error criterion.

The OS-Sato equalizer is implemented at the part of the transversal filter with the Sato algorithm in Figure 1, where the coefficient vector $\mathbf{c}(n)$ is nonlinearly adapted based on the order of the input sequence $x(n)$. Due to the OS operation, the impulse noise appears only on dominated elements of the coefficient vector and hence provides robustness against the impulse noise effect.

The OS-Sato equalizer prepares a coefficient matrix instead of a coefficient vector as follows

$$\mathbf{C}(n+1) = \begin{bmatrix} c_{0,0}(n) & c_{0,1}(n) & \cdots & c_{0,L-1}(n) \\ c_{1,0}(n) & c_{1,1}(n) & \cdots & c_{1,L-1}(n) \\ \cdot & \cdot & \cdot & \cdot \\ \cdot & \cdot & \cdot & \cdot \\ \cdot & \cdot & \cdot & \cdot \\ c_{L-1,0}(n) & c_{L-1,1}(n) & \cdots & c_{L-1,L-1}(n) \end{bmatrix}. \quad (8)$$

In (8), the elements $c_{i,j}(n)$,i, j=0, 1, $\cdots$, L-1 are initialized to zeros at n=0. For the adaptation of the OS-Sato equalizer, among the L by L elements of $\mathbf{C}(n)$, only L elements are selected using the OS operation of the input vector $\mathbf{x}(n)$ and then updated. Specifically, for the n^{th} iteration, only $c_{l(j),j}(n)$,j=0, 1, $\cdots$, L-1 are selected. And a coefficient vector

$$\mathbf{c}_{OS-Sato}(n) = [c_{l(0),0}(n), c_{l(1),1}(n), \cdots \cdots, c_{l(L-1),L-1}(n)]^T \quad (9)$$

is formed and updated where $l(j)$ corresponds to the order when the input vector, $\mathbf{x}(n) = [x(n), x(n-1), \cdot\cdot, x(n-L+1)(n)]^T$, is transformed into the OS vector as follows

$$\mathbf{S}(n) = [s_0(n), s_1(n), \cdots, s_{L-1}(n)]^T, \quad (10)$$

$$s_0(n) < s_1(n) < \cdot\cdot s_{L-1}(n). \quad (11)$$

The order $l(j)$ in (9) is determined for i, j=0, 1, $\cdot\cdot$ $\cdot$, $L-1$ by

$$l(j) = i \text{ if } s_i(n) = x(n-j). \quad (12)$$

The adaptation equations for the OS-Sato equalizer are given by

$$y(n) = \mathbf{x}(n)^T \mathbf{c}_{OS-Sato}(n), \quad (13)$$

$$e(n) = \hat{u}(n) - y(n) = \gamma sgn(y(n)) - y(n), \quad (14)$$

$$\mathbf{c}_{OS-Sato}(n+1) = \mathbf{c}_{OS-Sato}(n) + \mu e(n)\mathbf{x}(n). \quad (15)$$

The updated coefficient vector $\mathbf{c}_{OS-Sato}(n+1)$ is then inserted into the coefficient matrix $C(n+1)$. Such a process corresponds to one iteration for the OS-Sato equalizer.

4 THRESHOLD BASED BLIND EQUALIZATION

In this section, the threshold based adaptation for blind equalization is discussed.

To mitigate the impulse noise effect, the threshold based adaptation [16] is applicable to the Sato equalizer. The resulting equalizer is termed the threshold Sato (T-Sato) equalizer in this paper. The coefficient vector of the T-Sato equalizer will not be updated when an outlier is present in the input vector. This operation is equivalent to that the step size is set to zero in the above situations. Otherwise, the equalizer will update the coefficient vector using (5), (6) and (7). The no-adaptation combats the impulse noise effect.

The adaptive thresholding is also applicable to the OS-Sato equalizer, which results in the threshold OS-Sato (T-OS-Sato) equalizer. The coefficient vector of the T-OS-Sato equalizer is selected with the OS operation and updated with the threshold based adaptation using the Sato error criterion. If there is no outlier present in the input vector, the selected coefficient vector will be updated using (13), (14) and (15), and the impulse noise effect is suppressed by no-adaptation. In the T-Sato and T-OS-Sato equalizers, commonly the input signal corrupted by only the AWGN is effectively used for the equalizer coefficients adaptation.

The adaptive thresholding technique is described in details here. To implement the thresholding, the squared deviation $\Gamma(n)$ is calculated for each element of the input vector $\mathbf{x}(n)$ as

$$\Gamma(n) = [x(n) - \bar{x}(n)]^2, \quad (16)$$

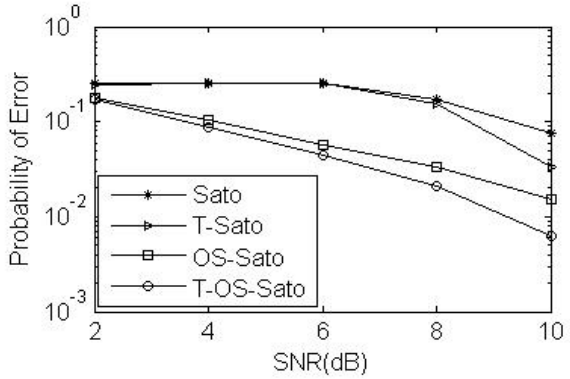

Figure 2: BER performance on $Channel$ 1 for noise generation model 1 with P_i=0.0001

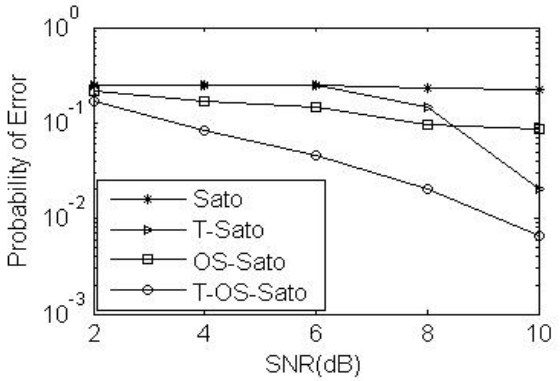

Figure 3: BER performance on $Channel$ 1 for noise generation model 1 with P_i=0.001

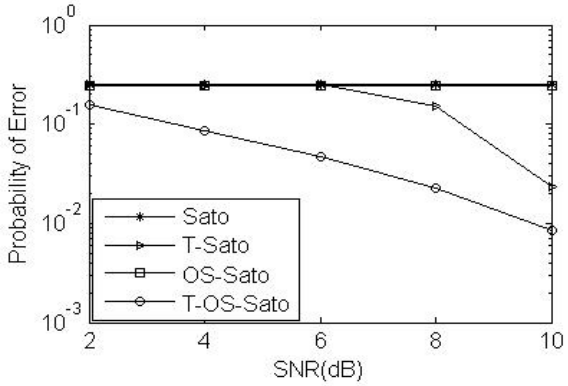

Figure 4: BER performance on $Channel$ 1 for noise generation model 1 with P_i=0.01

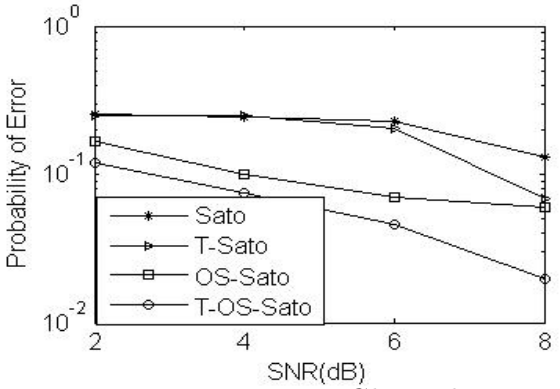

Figure 5: BER performance on $Channel$ 1 for noise generation model 2 with P_i=0.0001

where $\bar{x}(n)$ is the average up to the n^{th} input sample where the input samples corrupted by the AWGN only are used. This averaging is implemented so that it does not include potential impulse candidates. In general, observations having high order and low order are considered to be potential impulse candidates. Hence by eliminating the first and last elements, $s_0(n)$ and $s_{L-1}(n)$, of the OS vector, the influence of the impulse noise could be reduced. To deal with the AWGN only, by eliminating these two elements, $\bar{x}(n)$ is adaptively obtained as follows

$$\bar{x}(n) = \frac{1}{n+L-2}(n-1)\bar{x}(n-1) + \sum_{i=1}^{L-2} s_i(n)\cdot \tag{17}$$

The following threshold value is then evaluated to judge whether impulses are included in the input vector as

$$\Omega(n) = \alpha V(n), \tag{18}$$

where α is a scaling parameter and $V(n)$ is the estimate of the variance of the input signal corrupted by the AWGN only. $V(n)$ can be calculated adaptively as

$$V(n) = \frac{1}{n+L-2}[(V(n-1) + (\bar{x}(n-1))^2)(n-1) + \sum_{i=1}^{L-2} s_i(n)^2] - (\bar{x}(n))^2. \tag{19}$$

The squared deviation $\Gamma(n)$ is compared with the threshold value $\Omega(n)$. If

$$\Gamma(n) > \Omega(n), \tag{20}$$

then the observation is considered to be affected by impulse noise and the coefficient vector is not updated until the $(n+L-1)^{th}$ iteration. Otherwise, it will be updated. Rather than the trimming of high amplitude impulse noise in [11], the thresholding in (20) directly considers whether the observation is impulse or not. When the relationship in (20) is satisfied, it is expected that impulses are included in the input vector and they are then suppressed by no-adaptation.

5 NOISE GENERATION MODEL

Two different noise generation models are considered to verify the effectiveness of the OS-Sato, T-Sato and

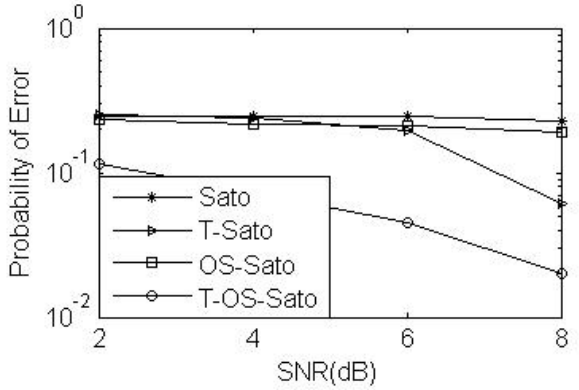

Figure 6: BER performance on $Channel$ 1 for noise generation model 2 with P_i=0.001

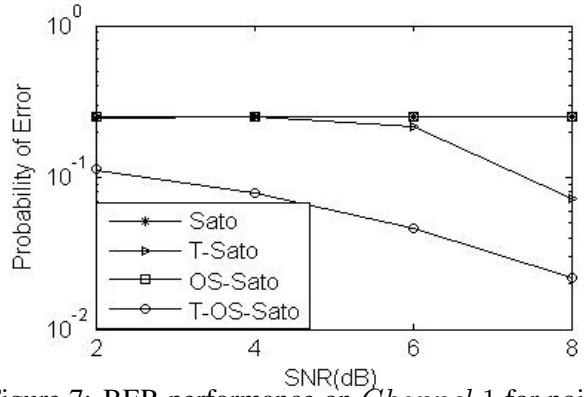

Figure 7: BER performance on $Channel$ 1 for noise generation model 2 with P_i=0.01

T-OS-Sato equalizers. For noise generation model 1, the impulse noise $I(n)$ is generated from a binary sequence with the values of $+10$, -10 and is added to the AWGN $g(n)$ to generate the white-impulse mixture noise $m(n)$. This model was used in [15].

For noise generation model 2, the Bernoulli-Gaussian model is considered to generate the white-impulse mixture noise $m(n)$. This model was used in [16][17]. In this model, $m(n)$ is given by

$$m(n) = S_g(n) + b(n)S_i(n) \tag{21}$$

where $b(n)$ is the Bernoulli process, that is, an independent and identically distributed sequence of zeros and ones with probability $P(b(n) = 1) = P_i$ which is the impulse noise generation probability. In (21), $S_g(n)$ and $S_i(n)$ are zero mean white Gaussian noises whose variances are v_g^2 and v_i^2, respectively. In this study, we choose the variance of the impulse noise as

$$v_i^2 = 50v_g^2. \tag{22}$$

Three different impulse noise generation probabilities, $P_i = 0.0001, 0.001$ and 0.01, are studied for both the noise generation models.

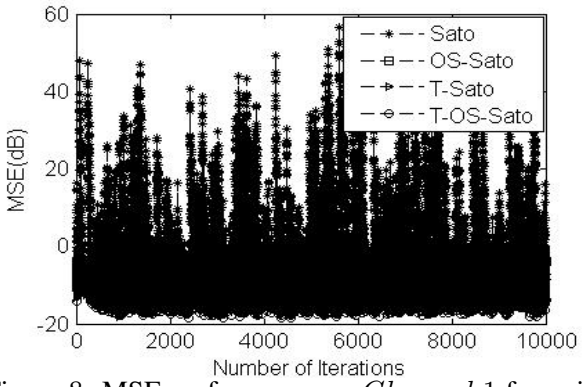

Figure 8: MSE performance on $Channel$ 1 for noise generation model 1 with P_i=0.001, SNR=20 dB and step size=0.13

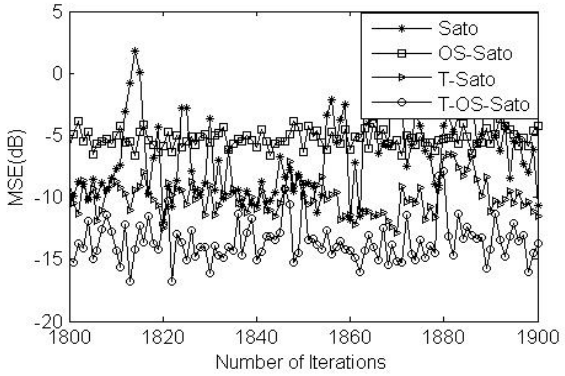

Figure 9: MSE performance on $Channel$ 1 for noise generation model 1 in enlarged view

6 SIMULATION RESULTS

The OS-Sato, T-Sato and T-OS-Sato equalizers are implemented and compared for simulation experiments. At first, we assume a minimum phase channel whose transfer function is given by

$$Channel\ 1\ : H(z) = 1 + 0.5z^{-1}. \tag{23}$$

The additive noise is a white-impulse mixture noise generated from noise generation models 1 and 2. The impulses are generated individually for each individual trial. The scaling parameter α in (18) is commonly set to 5.

Figures 2, 3 and 4 show the BER performance on $Channel$ 1 for noise generation model 1 with different P_i. The data number N=100000 is used. The equalizer length is set to L=4, the delay is zero and the step size is set to μ=0.04 commonly. Individual trials of 100 are implemented for each performance plot. From these figures, it is observed that the OS-Sato equalizer can suppress the impulse noise with lower P_i. On the other hand, the T-Sato equalizer can mitigate the impulse effect well for the entire P_i and it

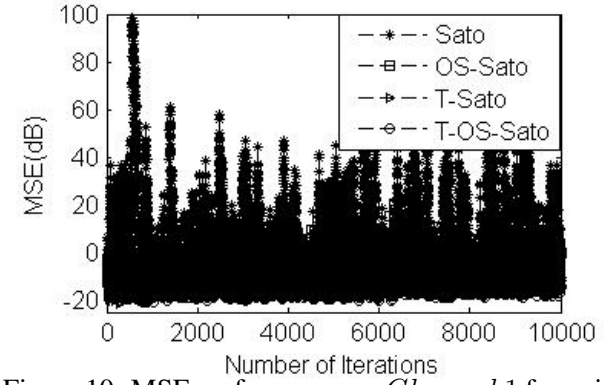

Figure 10: MSE performance on $Channel$ 1 for noise generation model 2 with P_i=0.001, SNR=20 dB and step size=0.155

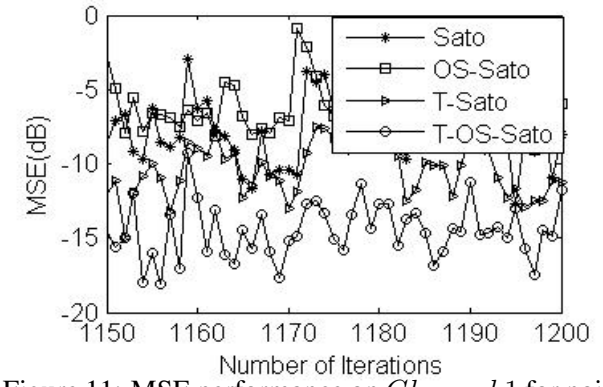

Figure 11: MSE performance on $Channel$ 1 for noise generation model 2 in enlarged view

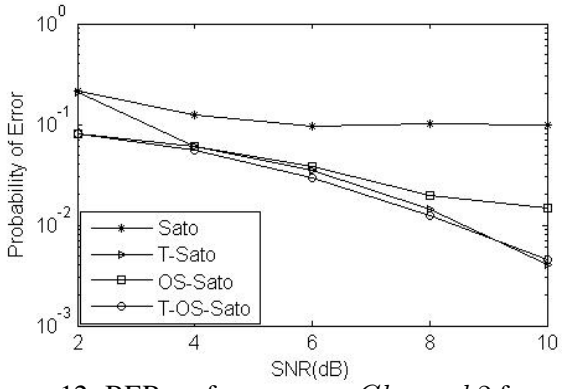

Figure 12: BER performance on $Channel$ 2 for noise generation model 1 with P_i=0.0001

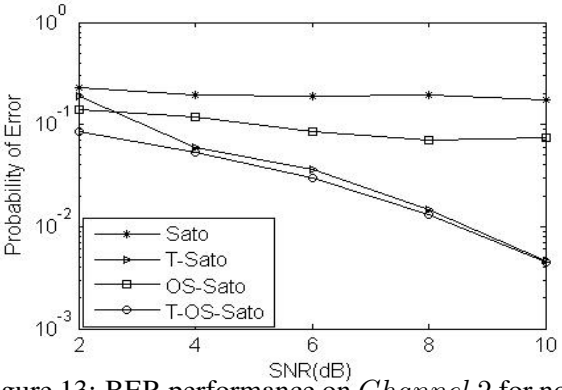

Figure 13: BER performance on $Channel$ 2 for noise generation model 1 with P_i=0.001

is effective in higher SNR conditions. Moreover, the T-OS-Sato equalizer outperforms for the entire P_i and for a wide range of SNR.

Figures 5, 6 and 7 show the BER performance on $Channel$ 1 for noise generation model 2 with different P_i. The data number N=100000 is used. The equalizer length is set to L=4, the delay is zero and the step size is set to μ=0.04 commonly. Individual trials of 100 are implemented for each performance plot. In Figures 5, 6 and 7, similar tendencies with those in Figures 2, 3 and 4 are observed.

The MSE performance on $Channel$ 1 for noise generation model 1 is shown in Figure 8 and an enlarged view of Figure 8 is shown in Figure 9, where P_i is set to a moderate value of 0.001, the SNR is set to 20 dB and the step size is set to 0.13 commonly. Individual trials of 100 are implemented for each plot. Figure 9 clearly demonstrates that the OS-Sato equalizer can suppress the impulse effect up to a certain level. The T-Sato equalizer provides successfully an MSE level with significant impulse noise suppression. The T-OS-Sato equalizer outperforms the other equalizers and provides a further MSE improvement of about 5 dB than the T-Sato equalizer. The MSE performance on $Channel$ 1 for noise generation model 2 is shown in Figure 10 and an enlarged view of Figure 10 is shown in Figure 11, where P_i is set to 0.001, the SNR is set to 20 dB and the step size is set to 0.155 commonly. Individual trials of 100 are implemented for each plot. Figure 11 also shows that the T-OS-Sato equalizer outperforms the other equalizers for noise generation model 2.

The performance of the OS-Sato, T-Sato and T-OS-Sato equalizers is investigated also on a raised cosine channel whose transfer function is given by

$$Channel\ 2\ : H(z) = \sum_{i=1}^{3} \frac{1}{2}(1 + cos\frac{2\pi(i-2)}{W})z^{-i}. \tag{24}$$

The parameter W is set to 3. Figures 12, 13 and 14 show the BER performance on $Channel$ 2 for noise generation model 1 with different P_i. The data number N=100000 is used. The equalizer length is set to L=7, the delay is 5 and the step size is set to μ=0.018 commonly. Individual trials of 100 are implemented for each performance plot. From Figures 12, 13 and 14, it is observed that the OS-Sato equalizer can sup-

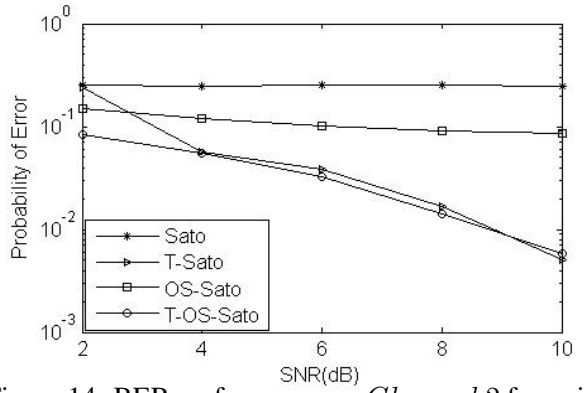

Figure 14: BER performance on $Channel$ 2 for noise generation model 1 with P_i=0.01

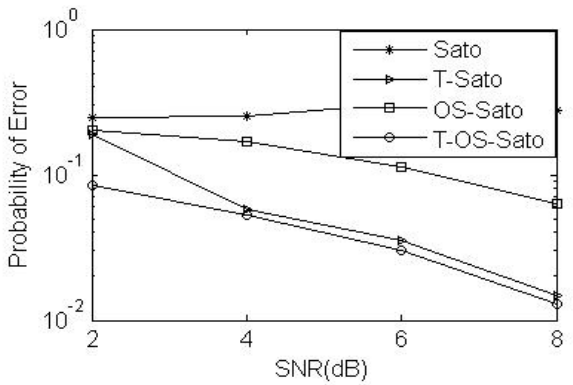

Figure 16: BER performance on $Channel$ 2 for noise generation model 2 with P_i=0.001

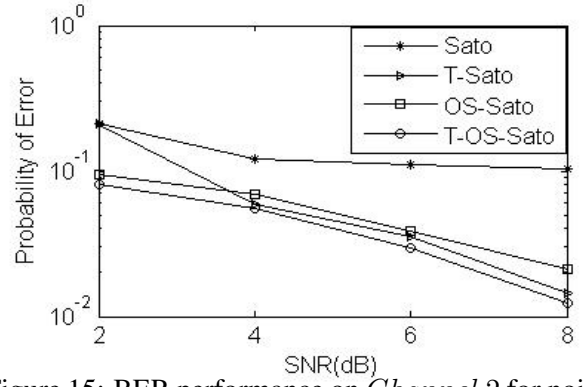

Figure 15: BER performance on $Channel$ 2 for noise generation model 2 with P_i=0.0001

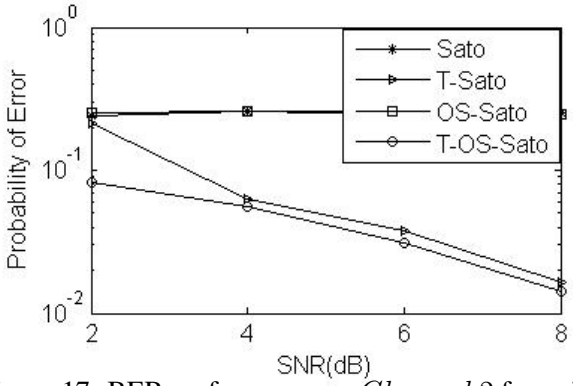

Figure 17: BER performance on $Channel$ 2 for noise generation model 2 with P_i=0.01

press the impulse noise for the entire P_i on $Channel$ 2. The OS-Sato equalizer is more effective with lower P_i. On the other hand, the T-Sato provides significant impulse noise suppression with higher P_i. The T-OS-Sato equalizer outperforms for the entire P_i and specifically in low SNR conditions on $Channel$ 2. Figures 15, 16 and 17 show the BER performance on $Channel$ 2 for noise generation model 2 with different P_i. The data number N=100000 is used. The equalizer length is set to L=7, the delay is 5 and the step size is set to μ=0.018 commonly. Individual trials of 100 are implemented for each performance plot. Similarly, it is observed that the impulse suppression is achieved more effectively with the T-OS-Sato equalizer for noise generation model 2 as well.

The MSE performance on $Channel$ 2 for noise generation model 1 is shown in Figure 18 and an enlarged view of Figure 18 is shown in Figure 19, where P_i is set to a moderate value of 0.001, the SNR is set to 20 dB and the step size is set to 0.13 commonly. Individual trials of 100 are implemented for each performance plot. Figure 19 shows that the OS-Sato equalizer can suppress the impulse noise up to a level on $Channel$ 2. Further MSE improvement is achieved with the T-Sato equalizer. The T-OS-Sato equalizer outperforms the other equalizers and provides a further 5 dB MSE improvement than the T-Sato equalizer on $Channel$ 2. The MSE performance on $Channel$ 2 for noise generation model 2 is shown in Figure 20 and an enlarged view of Figure 20 is shown in Figure 21, where P_i is set to 0.001, the SNR is set to 20 dB and the step size is set to 0.155 commonly. Individual trials of 100 are implemented for each performance plot. Figure 21 shows that similar MSE performances are achieved with the OS-Sato, T-Sato and T-OS-Sato equalizers, respectively for noise generation model 2 as well.

From the computer simulation results, it is observed that the OS based adaptation can suppress impulse noise up to a certain level. The threshold based adaptation can provide a further performance improvement. Finally, the combination of both can be the best solution to provide significant impulse noise suppression for the Sato equalizer.

7 Conclusion

This paper presents effective blind channel equalization in impulse noise environments. We provide novel

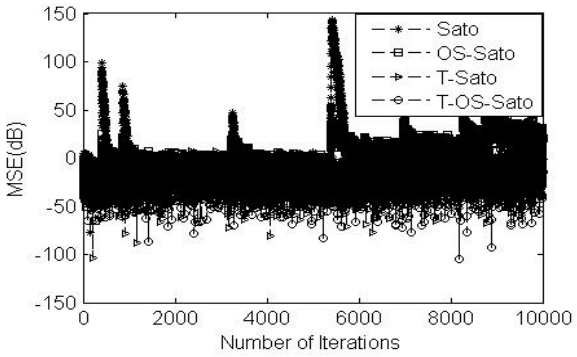

Figure 18: MSE performance on $Channel$ 2 for noise generation model 1 with P_i=0.001, SNR=20 dB and step size=0.13

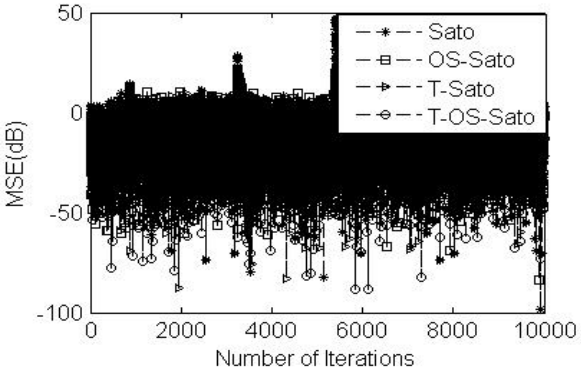

Figure 20: MSE performance on $Channel$ 2 for noise generation model 2 with P_i=0.001, SNR=20 dB and step size=0.155

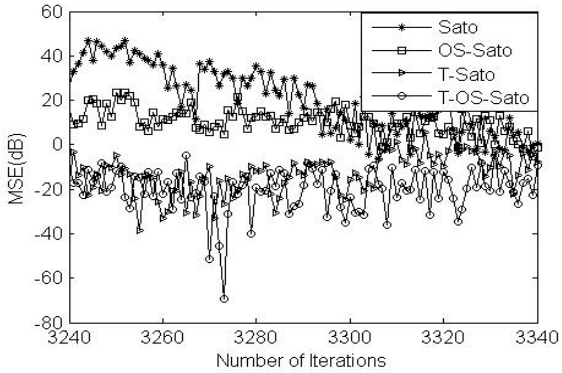

Figure 19: MSE performance on $Channel$ 2 for noise generation model 1 in enlarged view

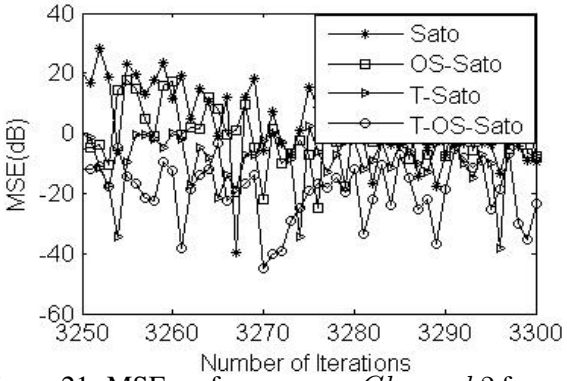

Figure 21: MSE performance on $Channel$ 2 for noise generation model 2 in enlarged view

insight of the OS operation for the Sato equalizer. The adaptive thresholding with the OS operation can significantly suppress the impulse noise regardless of its generation model and generation probability. Both BER and MSE measurements demonstrate the performance superiority of the T-OS-Sato equalizer in impulse noise environments for two different channels. Future work aims at automatic setting of the scaling parameter for the adaptive thresholding.

References:

[1] S.U.H. Qureshi, "Adaptive Equalization", $Proc.$ $IEEE$, Vol. 73, No.9, 1985, pp. 1349-1387.

[2] M.H. Wondimagegnhu, T. Shimamura and C.F.N. Cowan, "Frequency Domain Magnitude Banded LMS Algorithm for Equalization of Time Variant Multipath Channels", $WSEAS$ $Trans.$ on $Electronics$, Vol. 2, No. 1, 2005.

[3] Y. Jihong, C. Gang, X. Bin, W. Gaokui and H. Zishu, "An Effective Joint Implementation Design of Channel Equalizer and DDC for WDAR Receiver", $WSEAS$ $Trans.$ on $Signal$ $Processing$, Vol. 7, No. 1, 2011, pp. 12-22.

[4] A. Benveniste and M. Goursat, "Blind Equalizers", $IEEE$ $Trans.$ on $Communications$, Vol. COM-32, 1982, pp. 871-882.

[5] A.M. Nassar and W.E. Nahal, "Blind Equalization Technique for Cross Correlation Constant Modulus Algorithm (CC-CMA)", $WSEAS$ $Trans.$ on $Signal$ $Processing$, Vol. 6, No. 2, 2010, pp. 23-31.

[6] I. Pitas and A. N. Venetsanopoulos, "Adaptive Filters Based on Order Statistics", $IEEE$ $Trans.$ on $Signal$ $Process$, Vol. 39, No. 2, 1991, pp. 518-522.

[7] C.L. Nikias and M. Shao, $Signal$ $Processing$ $with$ $Alpha$ $-$ $Stable$ $Distributions$ and $Applications$, John Wiley & Sons, New York, 1996.

[8] A.Bovik, T.Hang, and D. Munson, "A Generalization of Median Filtering Using Combinations of Order Statistics", $IEEE$ $Trans.$ on $Acoustics$, $Speech$ and $Signal$ $Processing$, Vol. 31, 1983, pp. 1342-1350.

[9] F. Palmieri and C.G. Boncelet , "Ll-Filters-A New Class of Order Statistic Filters", $IEEE\ Trans.\ on\ Acoustics,\ Speech\ and\ Signal\ Processing$, Vol. 37, 1989, pp. 691-701.

[10] F. Palmieri and R.E. Croteau, "Adaptive Channel Equalization Using Generalized Order Statistic Filters",$IEEE\ Int.\ Conf.\ on\ Acoustics,\ Speech\ and\ Signal\ Processing$, Vol. 3, 1991, pp. 1933-1936.

[11] P.P. Gandhi and S.A. Kassam, "Design and Performance of Combination Filters for Signal Restoration", $IEEE\ Trans.\ on\ Signal\ Process$, Vol. 39, No. 7, 1991, pp. 1524-1540.

[12] E. Dubossarsky, S. Reisenfeld and T.R. Osborn, "Adaptive Channel Equalization With the Multirate Optimizing Order Statistics Equaliser (MOOSE)", $Global\ Telecommunications\ Conference$, Vol. 6, 1998, pp. 3509-3514.

[13] N. Kim, "Blind Signal Processing based on Information Theoretic Learning with Kernel-size Modification for Impulsive Noise Channel Equalization", $WSEAS\ Trans.\ on\ Communications$, Vol. 9, No. 7, 2010, pp. 418-428.

[14] Y. Sato, "A Method of Self-recovering Equalization for Multi-level Amplitude Modulation", $IEEE\ Trans.\ on\ Communications$, Vol. 23, 1975, pp. 679-682.

[15] Y. Morishita, Y. Tsuda, T. Fujii and T. Shimamura, "An LMS Adaptive Equalizer Using Threshold in Impulse Noise Environment", $IEEE\ Int.\ Conf.\ on\ Telecommunications$, Vol. 1, 2003, pp. 578-582.

[16] C.Y. Chi, J.M. Mendel and D. Hampson, "A Computationally Fast Approach to Maximum-likelihood Deconvolution", $Geophysics$, Vol. 49, No. 5, 1984, pp. 550-565.

[17] S.V. Zhidkov, "Impulsive Noise Suppression in OFDM Based Communication Systems", $IEEE\ Trans.\ on\ Consumer\ Electronics$, Vol. 49, No. 4, 2003, pp. 944-948.